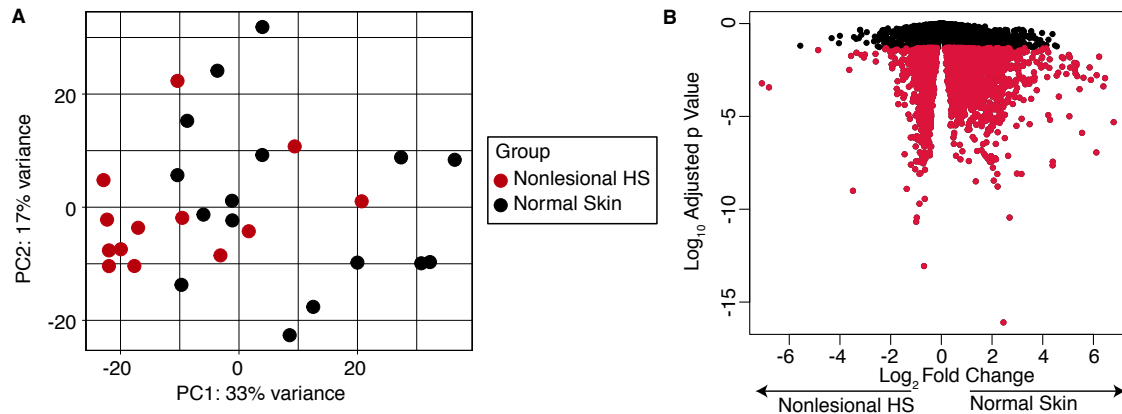
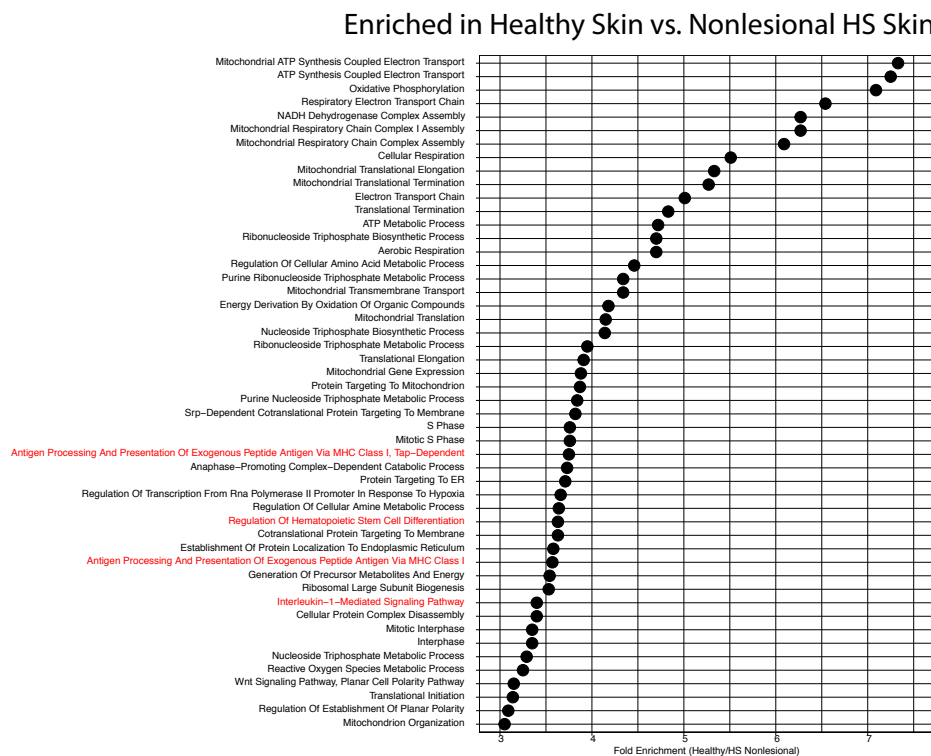


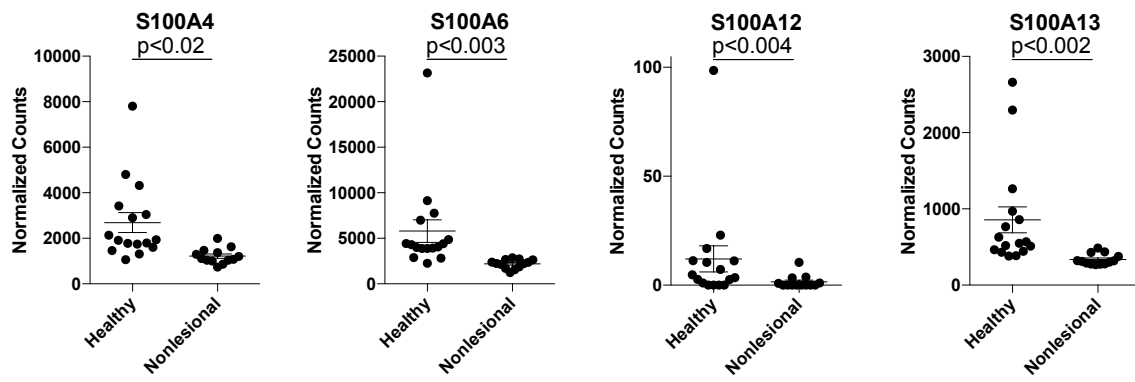
Supplemental Figures



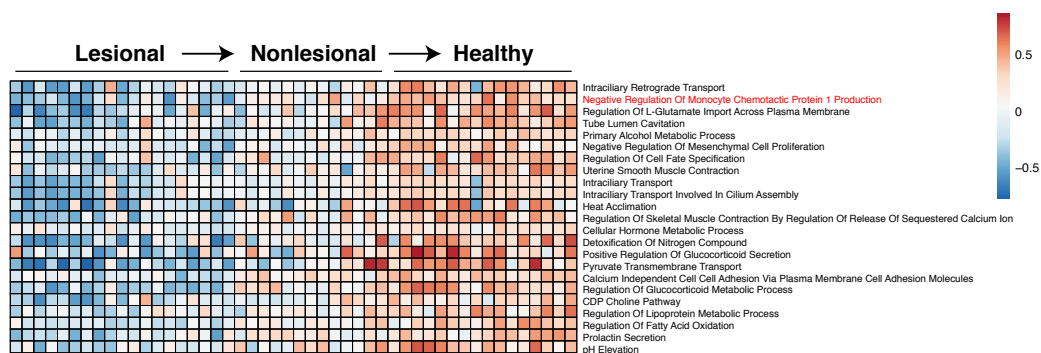
Supplemental Figure 1. **A.** Principal component analysis (PCA) of whole tissue RNA-Sequencing data from nonlesional HS skin and healthy control skin taken prior to initiation of anti-TNF. **B.** Volcano plot showing Log₂ Fold Change and Log₁₀ Adjusted P values comparing nonlesional skin to healthy control skin. Transcripts with adjusted p values <0.05 are colored in red.



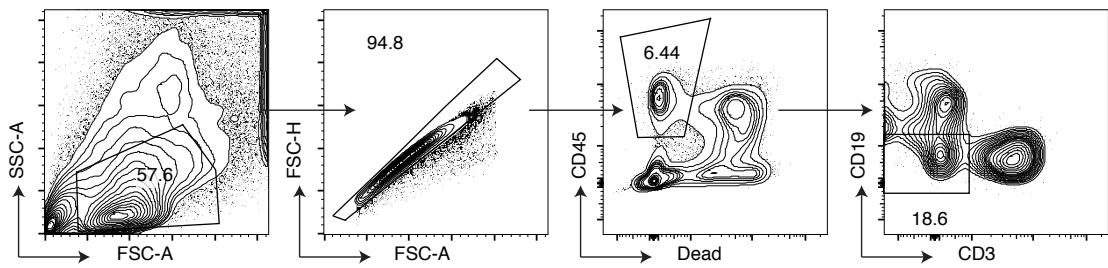
Supplemental Figure 2. The top 50 enriched (FDR<0.05) PANTHER Gene Ontology Pathways identified from genes significantly (adjusted p<0.05) increased in healthy control skin compared to pre-treatment nonlesional HS skin.



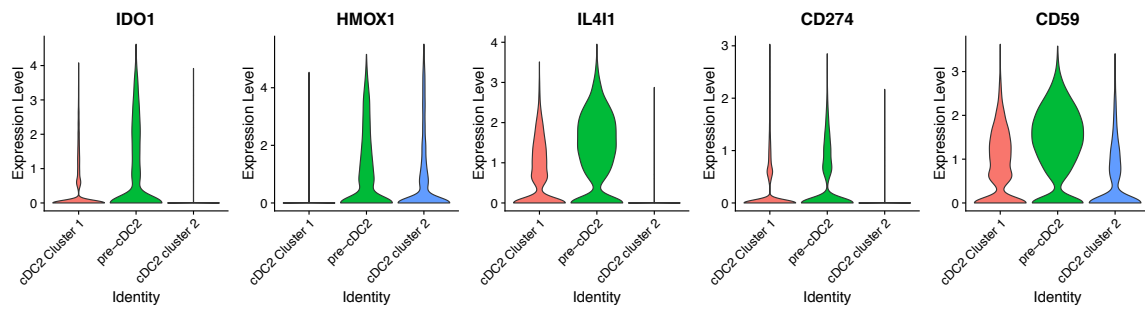
Supplemental Figure 3. Normalized counts for selected antimicrobial peptides in whole tissue RNA-Sequencing of healthy control skin and nonlesional HS skin prior to anti-TNF therapy (Wald test, DESeq).



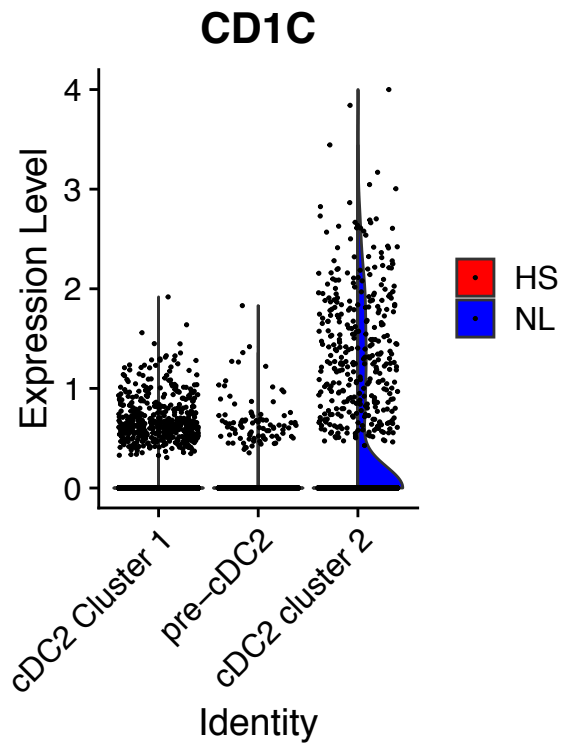
Supplemental Figure 4. GSVA enrichment scores of the union of Gene Ontology pathways significantly decreasing (adjusted p<0.05) in pre-treatment lesional HS skin versus pre-treatment nonlesional HS skin and pre-treatment nonlesional HS skin versus healthy control skin. Each column depicts an individual patient.



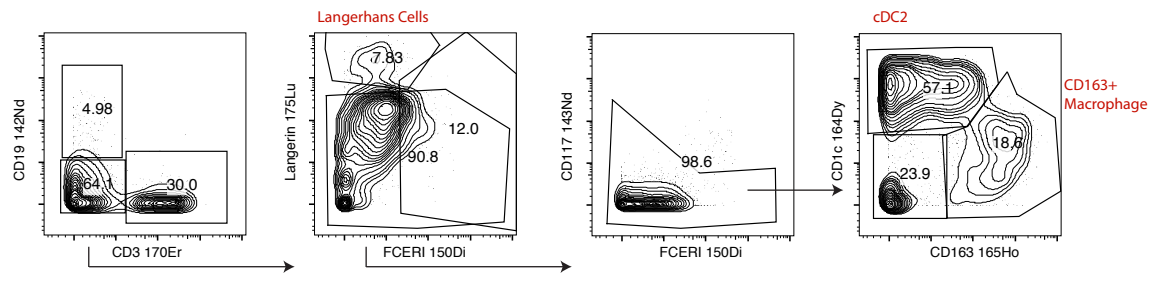
Supplemental Figure 5. Gating strategy for sort-purification of myeloid cells for single-cell RNASeq.



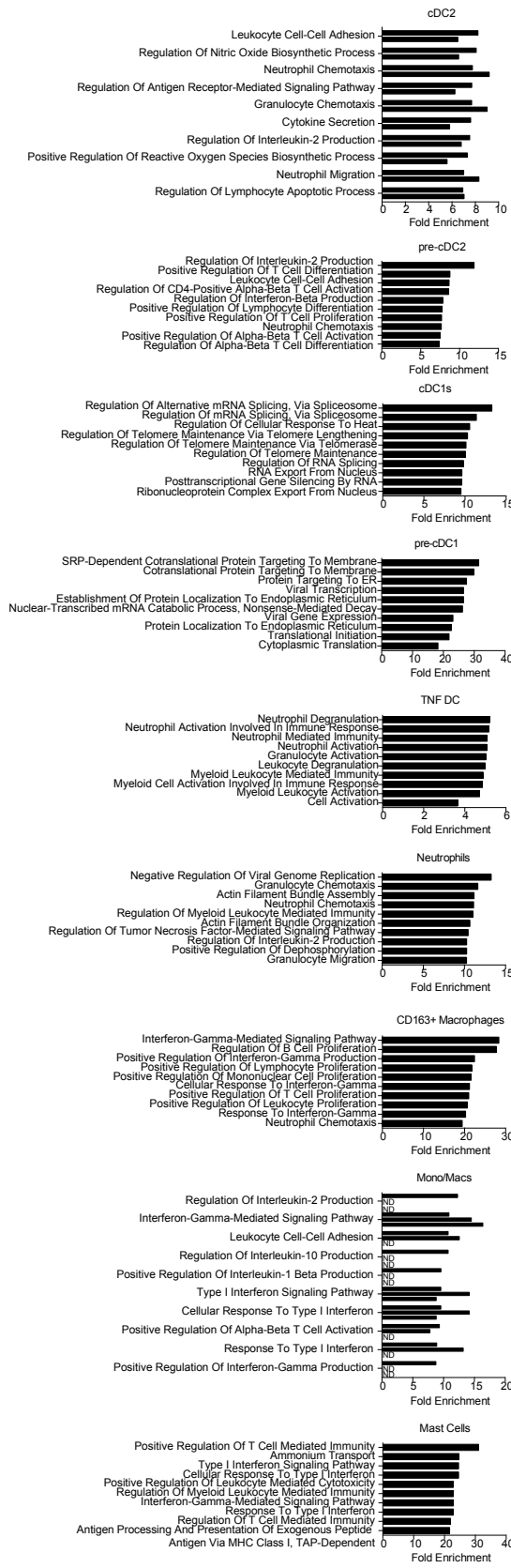
Supplemental Figure 6. Expression of IDO1, HMOX1, IL4I1, CD274 (PD-L1), and CD59 in scRNASeq data of myeloid cells of 2 HS skin samples and 2 healthy skin samples.



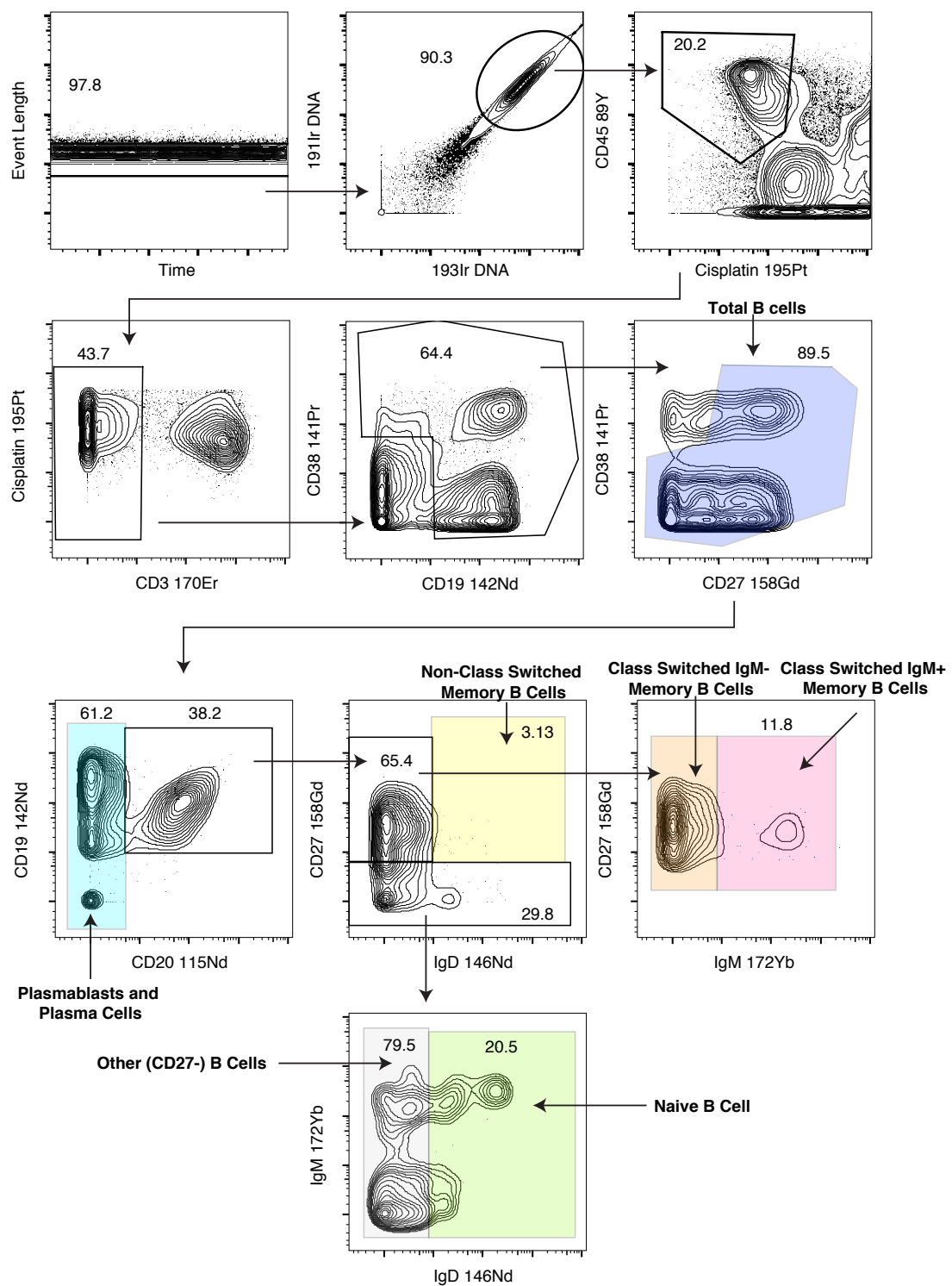
Supplemental Figure 7. CD1C expression on cDC2 and pre-cDC2 clusters in scRNASeq data of myeloid cells of 2 HS skin samples and 2 healthy skin samples.



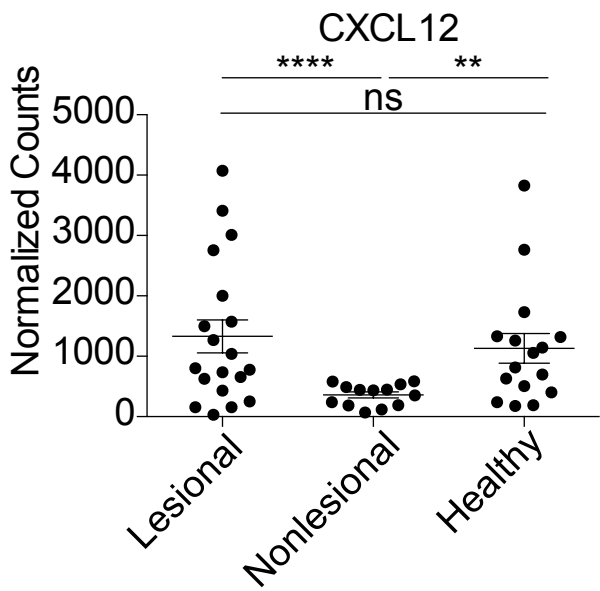
Supplemental Figure 8. Gating strategy for CyTOF analysis of myeloid cells.



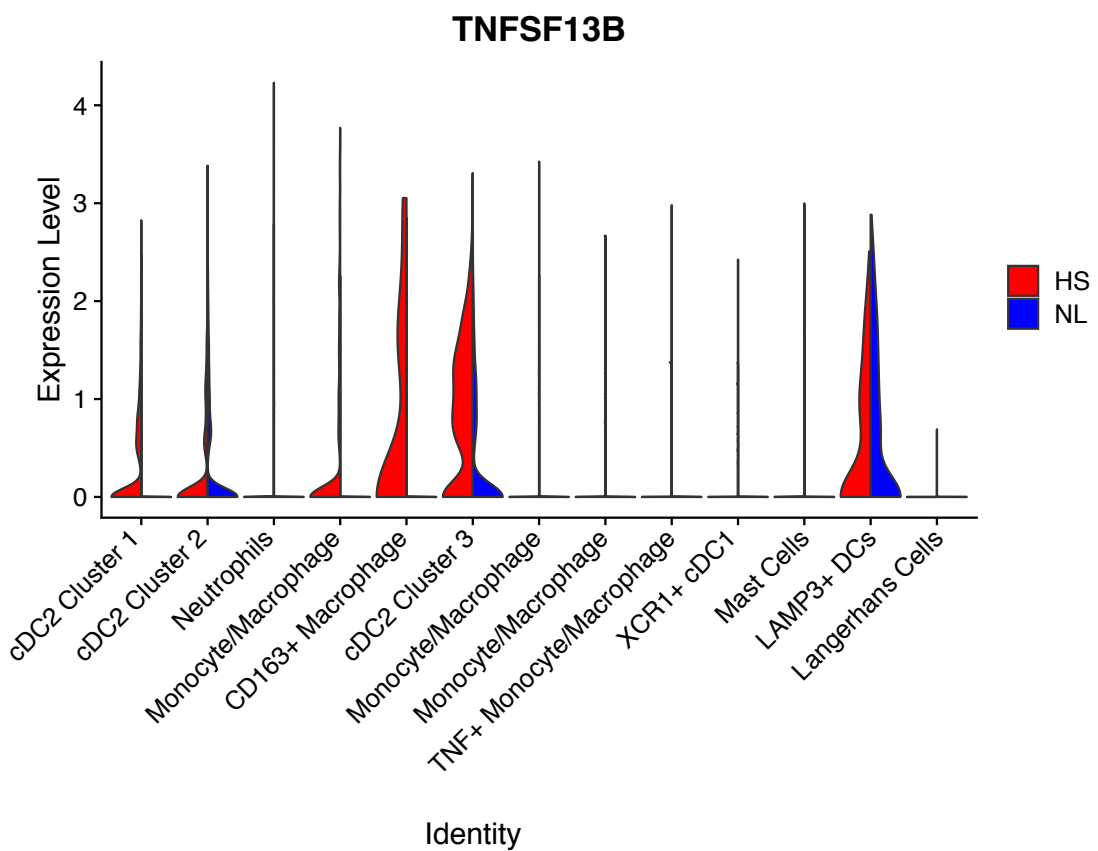
Supplemental Figure 9. Pathway analysis of differentially enriched genes within clusters of single cell RNA-seq data comparing healthy skin samples to HS end-stage disease.



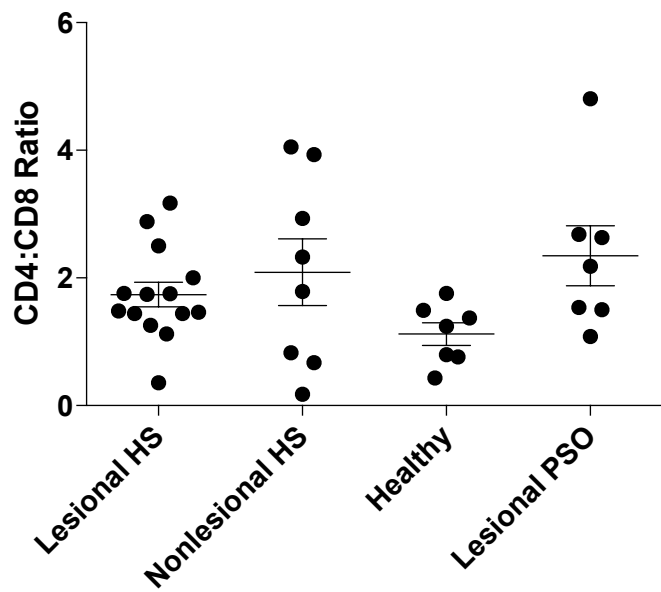
Supplemental Figure 10. Gating strategy for CyTOF analysis of B cells.



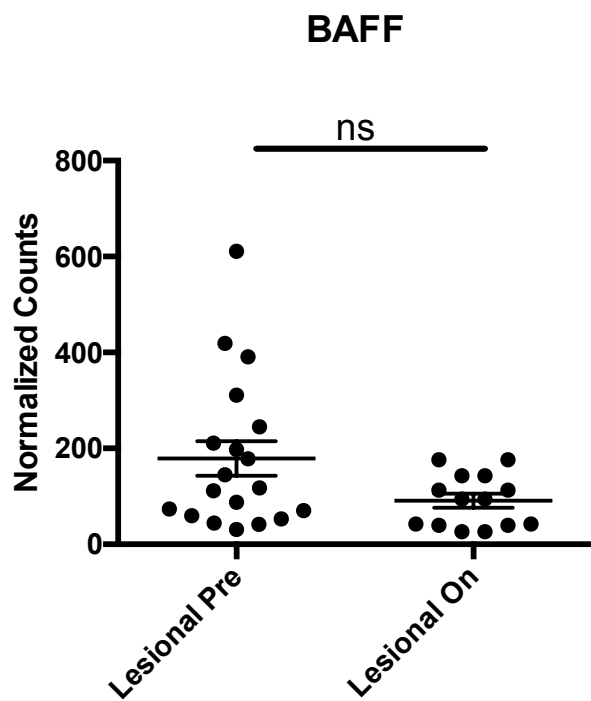
Supplemental Figure 11. Normalized counts for the gene CXCL12 in whole tissue RNA-Sequencing of lesional and nonlesional HS skin prior to anti-TNF therapy compared to healthy control skin (Wald test, DESeq).



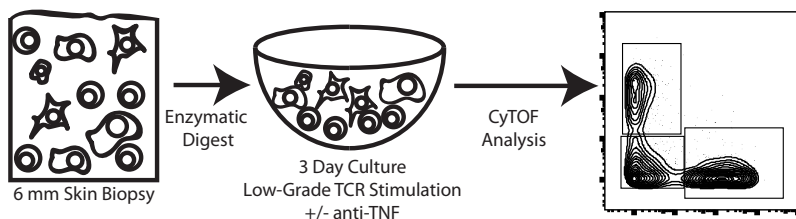
Supplemental Figure 12. Violin plots showing expression of TNFSF13B (corresponding to the protein BAFF) in myeloid clusters of scRNASeq data of two HS skin samples and two normal skin samples.



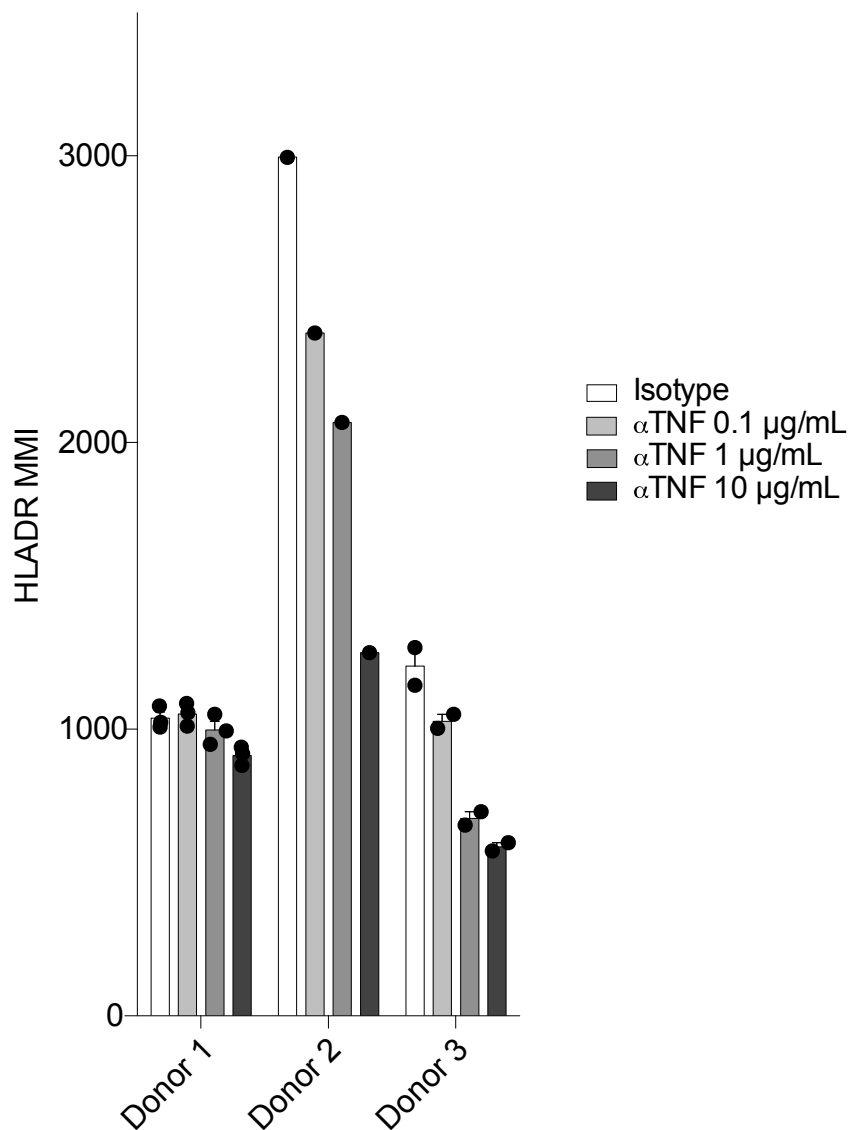
Supplemental Figure 13. Ratios of CD4 T cells to CD8 T cells within lesional HS, nonlesional HS, healthy control, and lesional psoriasis samples. One-way ANOVA, ns.



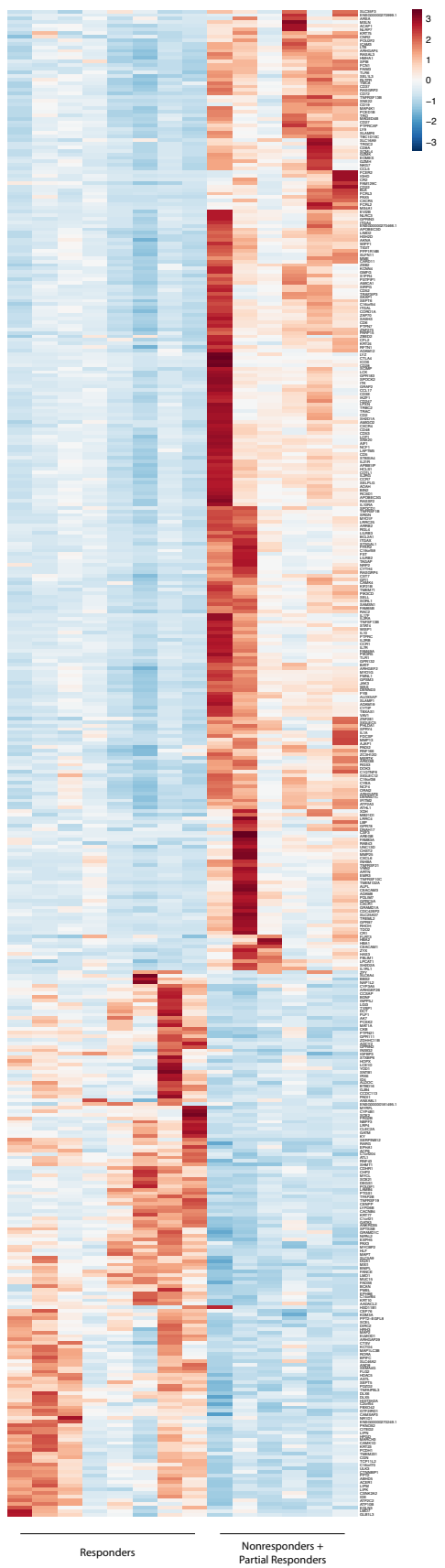
Supplemental Figure 14. Normalized counts of TNFSF13B, corresponding to the protein BAFF, transcript in lesional HS skin prior to anti-TNF therapy versus lesional HS skin from patients on anti-TNF therapy.



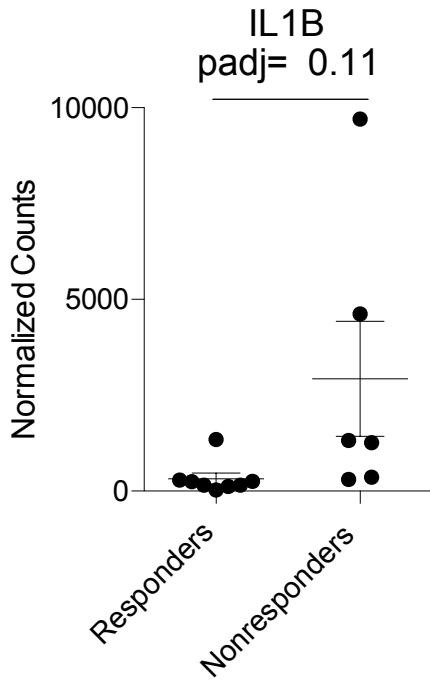
Supplemental Figure 15. Experimental design of HS ex vivo culture assays.



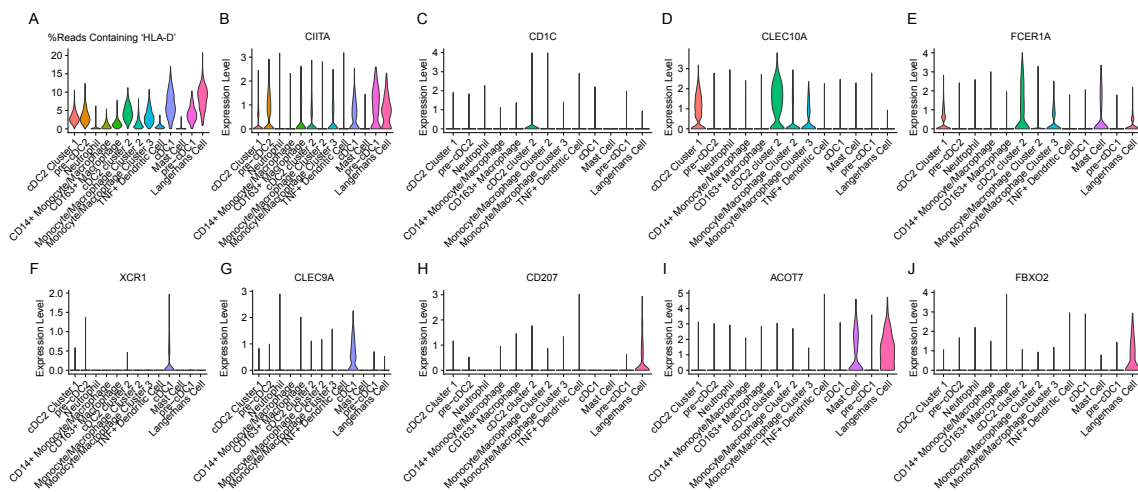
Supplemental Figure 16. HLADR Median Metal Intensity (MMI) on CD19+ B cells from HS skin after three days of culture with isotype control or increasing concentrations of anti-TNF antibody.



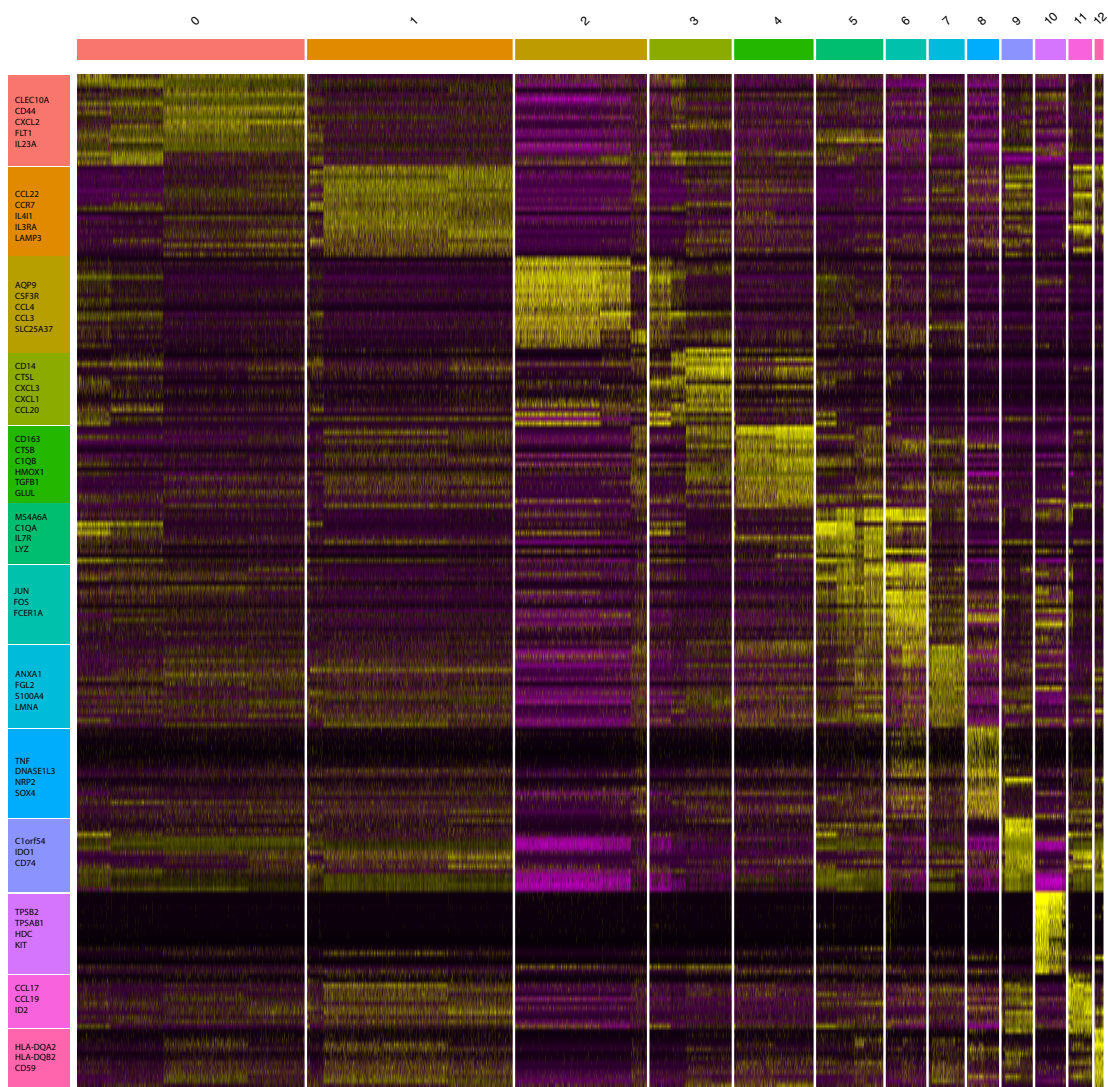
Supplemental Figure 17. Heatmap of genes significantly different between patients responding to anti-TNF α therapy versus those who did not (Wald test, adjusted p<0.05).



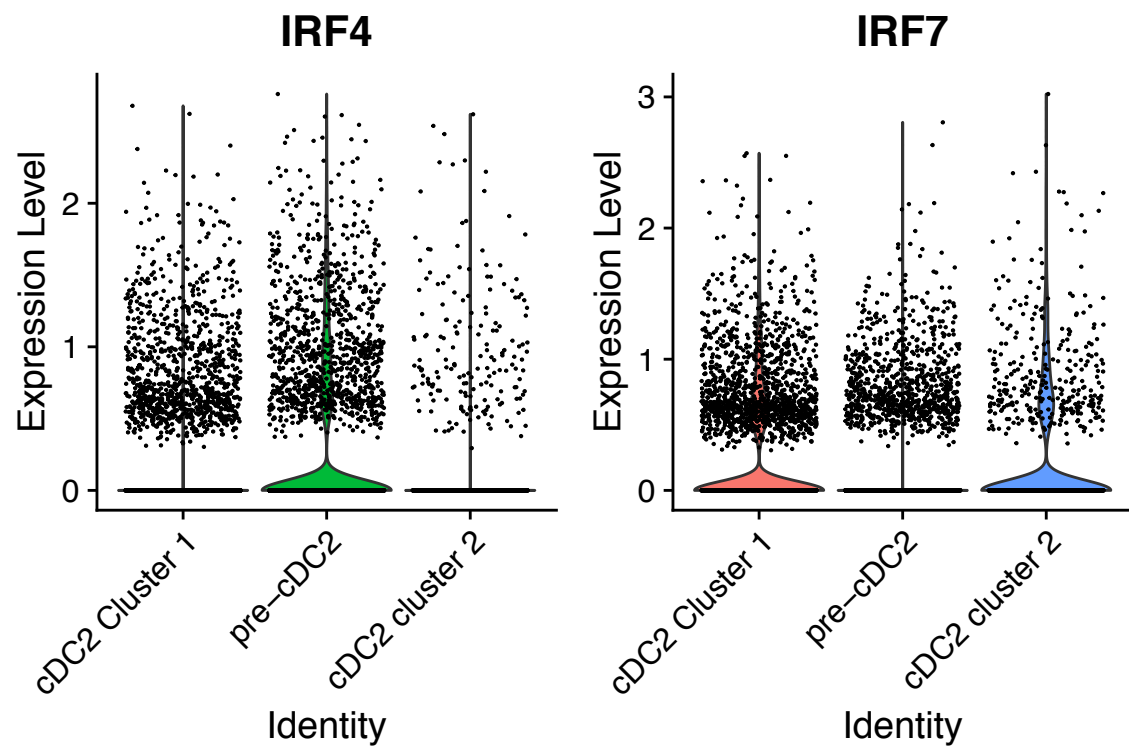
Supplemental Figure 18. Normalized counts for IL1B in whole tissue RNA-Sequencing comparing pre-treatment lesional skin of responders to anti-TNF therapy to non-responders (Wald test).



Supplemental Figure 19. Violin plots of combined scRNASeq data of myeloid cells from two HS skin samples and two healthy control skin samples showing (A) Expression of percentage of reads within cells matching the gene pattern 'HLA-D' (B) CIITA, (C)CD1C, (D)CLEC10A, (E)FCER1A, (F)XCR1, (G)CLEC9A, (H)CD207, (I) ACOT7, and (J) FBXO2.



Supplemental Figure 20. Heatmap of top twenty fold increased markers in scRNASeq data of myeloid cells for each cluster, with select genes annotated for each cluster.



Supplemental Figure 21. Violin plots of IRF4 (left) and IRF7 (right) expression on cDC2 and pre-cDC2 clusters in scRNASeq data of myeloid cells of 2 HS skin samples and 2 healthy skin samples.

Supplementary Table 1

Channel	Element	Protein	Clone	Vendor	Catalog No.
89	Y	CD45	H130	Fluidigm	3089003B
113	In				
115	In	CD20	2H7	BioLegend/UCSF conjugated	302302
139	La				
140	Ce				
141	Pr	CD38	EPR4106	Fluidigm	3141018D
142	Nd	CD19	HIB19	Fluidigm	3142001B
143	Nd	CD117	104D2	Fluidigm	3143001B
144	Nd	CD11b	ICRF44	Fluidigm	3144001B
145	Nd	CD4	RPA-T4	Fluidigm	3145001B
146	Nd	IgD	IA6-2	Fluidigm	3146005B
147	Sm	CD11c	BU15	Fluidigm	3147008B
148	Nd	CD14	RMO52	Fluidigm	3148010B
149	Sm	CD25	2A3	Fluidigm	3149010B
150	Nd	FCER1 γ -37 (CRA-1)		Fluidigm	3150027B
151	Eu				
152	Sm	gdTCR	11F2	Fluidigm	3152008B
153	Eu	CD8a	RPA-T8	BioLegend/UCSF conjugated	301002
154	Sm	CD24	ML5	BioLegend/UCSF conjugated	311102
155	Gd	CD56	B159	Fluidigm	3155008B
156	Gd	RORgt	REA278	Miltenyi/UCSF conjugated	130-108-059
157	Gd				
158	Gd	CD27	L128	Fluidigm	3158010B
159	Tb	PDL1	29E.2A3	Fluidigm	3159029B
160	Gd	Tbet	4B10	Fluidigm	3160010B
161	Dy	CD152 (CTLA-4)	14D3	Fluidigm	3161004B
162	Dy	Foxp3	PCH101	Fluidigm	3162011A
163	Dy	CD172a/b	SE5A5	Fluidigm	3163017B
164	Dy	CD1c	L161	BioLegend/UCSF conjugated	331502
165	Ho	CD163	GHI/61	Fluidigm	3165017B
166	Er	PD1	EH12.2H7	BioLegend/UCSF conjugated	329902
167	Er	Gata3	TWAJ	Fluidigm	3167007A
168	Er	Ki67	Ki67	Fluidigm	3168001B
169	Tm	CD138	DL-101	BioLegend/UCSF conjugated	352311
170	Er	CD3	UCHT1	Fluidigm	3170001B
171	Yb				
172	Yb	IgM	MHM-88	Fluidigm	3172004B
173	Yb	CD45RO	UCHL1	Fluidigm	3173016D
174	Yb	HLA-DR	L243	Fluidigm	3174001B
175	Lu	LANGERIN	4C7	Fluidigm	3175016B
176	Yb	CD127	A019D5	Fluidigm	3176004B
191/193	Ir	DNA intercalator			
195	Pt	Viability			
209	Bi	CD16	3G8	Fluidigm	3209002B

Supplementary Table 2

Antigen	Clone	Fluorophore	Vendor	Catalog Num	Notes
CD27	LG.7F9	PerCP-e710	eBioscience	46-0271-80	
CD4	S3.5	PE-Texas Red	Invitrogen	MHCDO417	
CD45	2D1	APC-eFluor780	eBioscience	47-9459-42	
CD8	RPA-T8	e605	eBioscience	93-0088-42	
CD3	SK7	BV711	Biolegend	344838	
CD3	SK7	PerCP	Biolegend	344814	Alternate
IL13	85BRD	FITC	eBioscience	11-7136-42	
TNF α	MAb11	PE-Cy7	BD	560923	
IL22	142928	PE	RND	IC7821P	
IFNg	4S.B3	Alexa700	Biolegend	502520	
IL17A	eBio64CAP17	e660	eBioscience	50-7178-41	
FOXP3	PCH101	e450	eBioscience	48-4776-42	

Methods

Hidradenitis Suppurativa Study Participants

Eligible participants were: 1) Age ≥ 18 years, 2) moderate-to-severe HS as defined by HS PGA score ≥ 3 , 2) active disease involving ≥ 1 body site, 3) 3 $t_{1/2}$ washout period from all systemic immunomodulating agents for management of HS at the pre-anti-TNF α time point. Exclusion criteria: 1) Pregnant or lactating female, 2) history of chronic or recurrent infection including HIV, hepatitis B or C, 3) diagnosis of primary or acquired immunodeficiency, 4) diagnosis of other active skin disease that would interfere with assessment of HS, 5) inability to give informed consent or have a parent/guardian who is willing to give informed consent.

Response to adalimumab was defined using the metric of achievement of Hidradenitis Suppurativa Clinical Response (HiSCR), which is a 50% reduction in overall abscess and nodule count with no increase in abscess count and no increase in draining fistula count. Partial responders were patients who reported improvement in disease course upon initiation of therapy (such as in pain, in number of new lesions, in number of flares), but did not meet criteria for a HiSCR response.

Surgical specimens received were deidentified and certified as Not Human Subjects Research.

Fresh 6mm skin punch biopsies were collected from inflammatory nodules (lesional) and normal-appearing skin in the same anatomic region 10cm away from the lesional tissue (nonlesional). The UCSF Institutional Review Board approved the proposed studies (16-19770).

For bulk RNASeq assays, 19 pre-anti-TNF α lesional skin biopsies, 13 pre-anti-TNF α nonlesional skin biopsies, 16 on-anti-TNF α lesional skin biopsies, and 16 control skin samples were profiled. For CyTOF analysis, 12 lesional HS skin biopsies (10 of which were pre-anti-TNF α), 18 surgical HS excisions, and 14 control skin samples were profiled. For flow cytometry analysis, 14 pre-anti-TNF α lesional HS samples, 8 pre-anti-TNF α nonlesional HS samples, 10 on-anti-TNF α lesional skin biopsies, and 7 healthy skin samples were profiled.

Psoriatic Study Participants

Conventional psoriasis patient samples and site-matched healthy controls were previously reported on in Ahn et al (28).

Whole Tissue RNA-Sequencing

Human skin from 16 healthy donors resulting from surgical discards taken from the armpit or groin and approximately half of one 6 mm punch biopsy from lesional and nonlesional skin of donors with hidradenitis suppurativa were placed in RNAlater overnight at 4° Celsius before banking at -80° Celsius prior to processing. RNA isolation and sequencing was performed by Expression Analysis (Morrisville, NC) in four batches. Isolation was performed with Qiagen RNeasy Spin Columns. RNA was quantified via Nanodrop ND-8000 spectrophotometer, and quality was checked by Agilent Bioanalyzer Pico Chip. cDNA was created from 100 ng of input RNA with the TruSeq Stranded mRNA input kit (50bp, paired end stranded reads) and was sequenced to a 25M read depth. Reads were aligned to Ensembl hg19 GRCh37.75 reference genome with kallisto software (v. 0.46.0) using the bootstrap=40 setting (82). Fastq files from the 8 conventional psoriasis samples and 9 control samples were aligned by the same method.

Bioinformatic Analysis

Differential expression was determined using the R/Bioconductor package DESeq2 (v. 1.26.0) (84) in R version 3.6.1. PCA plots were generated with the DESeq2::plotPCA command with the default settings on variance-stabilizing transformed data. Patient response data was corrected for patient PGA score and batch. A PANTHER (85) statistical overrepresentation test was performed using the PANTHER webtool on significantly increased (adjusted p<0.05) transcripts comparing lesional skin of patients prior to anti-TNF α therapy to healthy skin (See Supplementary Table 3). Statistical overrepresentation for PSO samples utilized site-matched controls from the previously published dataset. Gene Ontology complete biological processes were tested for enrichment using the Fisher's exact test, with False Discovery Rate <0.05 considered significant. Ingenuity Pathway Analysis was conducted on differentially expressed genes (adjusted p<0.05, log2 fold change +/- 2) comparing lesional skin of patients prior to anti-TNF α therapy to healthy skin, with upstream regulators increased or decreased with an adjusted p value <0.05 considered significant. Gene Set Variation Analysis was conducted using the R package GSVA (v. 1.34.0) and GSEABase (v. 1.48.0) (29). Individual patient samples were scored for pathway enrichment using Broad Institute C5 gene set collection (v7.0) (86-88), and differential enrichment scores between lesional skin of patients prior to anti-TNF α therapy versus healthy skin were tested with the limma package (v. 3.42.1), with p<0.05 being considered significant using the Benjamini-Hochberg correction. Cell type enrichment analysis of FPKM normalized bulk RNA-sequencing data was performed using the xCell webtool (32). xCell scores were obtained using the default matrix of categorical cell type signature scores (n=64).

Tissue Processing

Single cell suspensions of punch biopsies and surgical excisions were obtained by overnight digestion. Samples were mechanically minced with scissors and incubated at

37° Celsius in a tissue culture incubator overnight in RPMI with 10% FBS with collagenase IV (0.8 mg/mL, Worthington, Cat# LS004186) and DNase (20 µg/mL, Sigma, Cat# DN251G). Following incubation, sample digestion was quenched with RPMI and 10%FBS, and samples were filtered, centrifuged, washed, and counted with a Nucleocounter NC-200 (ChemoMetec) prior to downstream experiments.

Single Cell RNASequencing

Surgical excisions and healthy control samples were dermatomed at a 1000 micron depth prior to overnight digestions. Single cell suspensions of the dermis of two HS surgical excisions and two healthy control samples were stained with anti-CD3, anti-CD19, and viability dye prior to sorting using a BD Aria II. Samples for single cell were unable to be gender matched due to processes in sample de-identification. Myeloid cells (Live, singlet, CD3-, CD19- events) were sort-purified, counted, and loaded onto a 10x Single Cell 3'v3 GEMS chip and sequenced by the 10x Genomics Core (UCSF). Fastq files were aligned to GRCh38 with Cell Ranger version 3.0.2. Clustering and differential expression analysis was performed using the R package Seurat (v3.1.2) (98). Genes expressed in <3 cells were removed, and cells were filtered in Seurat for each sample with cutoffs of >200 and <3000 RNA features per cell and <5% of mitochondrial genes. Data was normalized and variable features were identified with the Seurat commands with 2000 variable features used with the vst selection method. Data from the four samples was integrated, data was scaled, PCA/UMAP were run, and neighbors identified based upon 35 dimensions of data. Clusters were identified at a resolution of 0.5. For Figure 3, clusters of NK/T cells which could not be deconvoluted bioinformatically and a cluster of contaminating fibroblasts were removed. Figure 6 contains data from all cells which passed the initial Seurat cutoffs. Differential expression was performed using the Seurat FindMarkers command with Wilcoxon rank sum test comparing HS sample clusters to Healthy Skin sample clusters.

scRNASeq Myeloid Cluster Determination

Fibroblast and endothelial contaminants, B cell contaminants, and a cluster of NK cells that could not be transcriptionally distinguished from CD3⁺ contaminants were excluded from analysis. Based on percentages of Class II HLA molecules reads within cells, Clusters 0, 1, 5, 8, 9, 11 and 12 were presumed to be more likely to be of the dendritic cell lineage (Supplemental Fig. 19A, 19B).

Clusters 0 and 5 were designated as clusters of cDC2 dendritic cells due to high CLEC10A expression and presence of CD1C and FCER1A expression (Supplemental Fig. 19C-E) (90,91).

Cluster 1 was identified as a unique cluster of pre-cDC2s. Pre-cDCs have recently been described in the literature (38) as bearing intermediate signatures between plasmacytoid dendritic cells and conventional dendritic cells. IL3RA expression was high in this cluster (Supplemental Fig. 20). Class II machinery (HLA-D molecules and CIITA) was greater than has been reported for plasmacytoid dendritic cells (Supplemental Fig. 19A,19B) (92), and IRF4 expression predominated over IRF7 (Supplemental Fig. 21) (93). This cluster was positioned intermediate between the other two cDC2 clusters identified (Figure 3A). This cluster expressed immunosuppressive effector molecules HMOX1, IDO1, IL4I1, CD274 (PDL1) and CD59 (Supplemental Fig. 6).

Cluster 2 was designated as neutrophils due to high AQP9 expression (94) and high expression of CSF3R (95).

Cluster 3, 4, 6, and 7 were determined to be of macrophage lineage. Cluster 3 was determined to be a monocyte derived macrophage population due unique expression of CD14. Cluster 4 was designated as CD163⁺ Macrophages due to high CD163, MRC1 (CD206), and GLUL expression. Both clusters 3 and 4 had high expression of macrophage markers MARCO and C1QA. Cluster 6 expressed high levels of JUN and FOS. Cluster 7 expressed high levels of ANXA1 and FGL2. (Supplemental Fig. 20).

Cluster 8 expressed high TNF transcript, DNASE1L3, NRP2, and SOX4 (Supplemental Fig. 20).

Cluster 9 was designated as type 1 conventional dendritic cells due to high XCR1 and CLEC9A expression (Supplemental Fig. 19F, 19G).

Cluster 10 was designated as mast cells due to high expression of TPSB2, TPSAB1, KIT, MAOB, and HDC (Supplemental Fig. 20).

Cluster 11 was designated as pre-cDC1 due to overlap in marker expression with Cluster 9 but lower degree of XCR1 and CLEC9A expression compared to cluster 9 (Supplemental Fig. 19F, 19G, 20).

Cluster 12 was determined to be Langerhans cells due expression of Langerin and genes ACOT7 and FBXO2 (Supplemental Fig. 20).

Mass Cytometry

Single cell suspensions were washed with 5 mM EDTA-PBS and centrifuged at 600 g for 5 minutes at 4 °C. Cells were then resuspended in equal volumes of 5 mM EDTA-PBS and 50 uM cisplatin (Sigma, P4394) for viability determination for 1 minute at room temperature (RT) before quenching with 5 mM EDTA-PBS with 0.5% BSA. After centrifugation, cells were fixed with 1.6% PFA in PBS with 0.5% BSA and 5 mM EDTA for 10 minutes at RT and then washed twice with PBS. Cells were then resuspended in PBS with 0.5% BSA and 10% DMSO and stored at -80 °C. Prior to staining, cells were left to thaw at RT and washed in Cell Staining Media (CSM, PBS with 0.5% BSA and 0.02% NaN3) and then vortexed with FC Receptor Blocking Solution (BioLegend, Cat# 422302). 300,000 cells per sample were barcoded with the Cell-ID 20-Plex Pd Barcoding Kit (Fluidigm) kit and then combined for staining. CD138, CD24, CD1c, CD20, PD1, RORyt, and CD8a antibodies were metal-conjugated at the UCSF Parnassus Flow Cytometry Core using Maxpar Antibody Labeling Kits (Fluidigm). All other metal conjugated antibodies were obtained from Fluidigm. Antibodies are listed in

Supplementary Table 1. Cells were stained in an extracellular antibody cocktail for 30 minutes at RT on a shaker and then washed with CSM. Cells were then permeabilized with the Foxp3/Transcription Factor Staining Buffer Set (eBioscience, 00-5523-00) for 30 minutes at RT on a shaker and then washed twice with Permeabilization Buffer (eBioscience, 00-8333-56) before staining in an intracellular antibody cocktail for 1 hour at RT on a shaker. Following intracellular staining, cells were washed once with Permeabilization Buffer and once with CSM, and then resuspended in PBS with 1.6% PFA and 100 nM Cell-ID Intercalator-Ir (Fluidigm, 201192B) and kept at 4 °C. Before data acquisition, cells were washed sequentially in CSM, PBS, and MilliQ H₂O. Cells were then resuspended in MilliQ H₂O containing EQ Four Elements Calibration Beads (Fluidigm, Cat# 201078) and analyzed with a CyTOF2 Mass Cytometer (Fluidigm). Mass cytometry files were normalized to the bead standards in R (3.6.1) using the premessa package (0.2.4, github.com/ParkerICL/premessa). Analysis was performed on viable singlets as determined by the iridium, event length, and cisplatin channels. UMAP visualizations were generated with the CATALYST package (1.10.1) (96).

Ex vivo Culture

Ex vivo culture experiments were performed on single cell suspensions of HS skin by incubating 300,000 cells with suboptimal TCR stimulation (0.1 µg/mL anti-CD3/28, plate-bound) for three days in media (RPMI + 10%FBS + glutamine + penicillin/streptomycin + non-essential amino acids). Tested conditions included an increasing range of anti-TNF α (0.1, 1, 10 µg/mL, AbbVie) or isotype control (10 µg/mL, AbbVie). Following incubation, cells were stained with cisplatin viability reagent, fixed with 1%PFA, and banked for CyTOF. For each CyTOF run, samples were barcoded and batched together, with all tested conditions contained in one run. CyTOF samples were normalized and debarcoded with Premessa, and were analyzed in Flowjo X and CATALYST.

Flow Cytometry

Samples were stimulated with Cell Stimulation Cocktail (Tonbo Biosciences, catalog no. TNB-4975) for four hours at 37 °C, and then were stained for surface antigens and a live/dead marker (Ghost Dye Violet 510, Tonbo Biosciences) in FACS buffer (PBS with 2% fetal bovine serum) for 30 min at 4°C. Cells were then fixed and permeabilized using the FOXP3-staining buffer kit (eBioscience) for 30 minutes at 4°C, and then stained intracellularly for 30 minutes at 4°C before being washed and resuspended in FACS buffer. Antibodies used are listed Supplementary Table 2. CD8 T cells were gated as live, singlet, CD45⁺, CD3⁺, CD8⁺, CD4⁻. CD4 Tcon cells were gated as live, singlet, CD45⁺, CD3⁺, CD8⁻, FOXP3⁻. Tregs were gated as live, singlet, CD45⁺, CD3⁺, CD8⁻, FOXP3⁺. Samples were acquired on a Fortessa (BD Biosciences) in the UCSF Flow Cytometry Core. FlowJo software (FlowJo LLC) was used to analyze flow cytometry data. Psoriatic samples were collected contemporaneously with HS samples and have been described in a previous publication (32).

Histology

Biopsies from a subset of HS patients were partitioned and approximately one quarter of a 6mm punch biopsy was placed in a cassette in 10% formalin, followed by transfer to 70% ethanol after 24 hours. Samples were embedded in paraffin, sectioned, and stained with hematoxylin and eosin by the UCSF Dermatopathology Core.

References

84. M. I. Love, W. Huber, S. Anders, Moderated estimation of fold change and dispersion for RNA-seq data with DESeq2, *Genome Biol.* **15**, 550–8 (2014).
85. H. Mi, A. Muruganujan, D. Ebert, X. Huang, P. D. Thomas, PANTHER version 14: more genomes, a new PANTHER GO-slim and improvements in enrichment analysis tools, *Nucleic Acids Res* **47**, D419–D426 (2019).
86. A. Subramanian, P. Tamayo, V. K. Mootha, S. Mukherjee, B. L. Ebert, M. A. Gillette, A. Paulovich, S. L. Pomeroy, T. R. Golub, E. S. Lander, J. P. Mesirov, Gene set

- enrichment analysis: a knowledge-based approach for interpreting genome-wide expression profiles, *Proc.Natl.Acad.Sci.U.S.A.* **102**, 15545–15550 (2005).
86. M. Ashburner, C. A. Ball, J. A. Blake, D. Botstein, H. Butler, J. M. Cherry, A. P. Davis, K. Dolinski, S. S. Dwight, J. T. Eppig, M. A. Harris, D. P. Hill, L. Issel-Tarver, A. Kasarskis, S. Lewis, J. C. Matese, J. E. Richardson, M. Ringwald, G. M. Rubin, G. Sherlock, Gene Ontology: tool for the unification of biology, *Nat Genet* **25**, 25–29 (2000).
88. The Gene Ontology Resource: 20 years and still GOing strong, *Nucleic Acids Res* **47**, D330–D338 (2019).
89. T. Stuart, A. Butler, P. Hoffman, C. Hafemeister, E. Papalexi, W. M. Mauck, Y. Hao, M. Stoeckius, P. Smibert, R. Satija, Comprehensive Integration of Single-Cell Data, *Cell* **177**, 1888-1902.e21 (2019).
90. L. Heger, S. Balk, J. J. Lühr, G. F. Heidkamp, C. H. K. Lehmann, L. Hatscher, A. Purbojo, A. Hartmann, F. Garcia-Martin, S.-I. Nishimura, R. Cesnjevar, F. Nimmerjahn, D. Dudziak, CLEC10A Is a Specific Marker for Human CD1c+ Dendritic Cells and Enhances Their Toll-Like Receptor 7/8-Induced Cytokine Secretion, *Front Immunol* **9** (2018), doi:10.3389/fimmu.2018.00744.
91. M. Durand, T. Walter, T. Pirnay, T. Naessens, P. Gueguen, C. Goudot, S. Lameiras, Q. Chang, N. Talaei, O. Ornatsky, T. Vassilevskaia, S. Baulande, S. Amigorena, E. Segura, Human lymphoid organ cDC2 and macrophages play complementary roles in T follicular helper responses, *J Exp Med* **216**, 1561–1581 (2019).
92. the Immunological Genome Consortium, J. C. Miller, B. D. Brown, T. Shay, E. L. Gautier, V. Jojic, A. Cohain, G. Pandey, M. Leboeuf, K. G. Elpek, J. Helft, D. Hashimoto, A. Chow, J. Price, M. Greter, M. Bogunovic, A. Bellemare-Pelletier, P. S. Frenette, G. J. Randolph, S. J. Turley, M. Merad, Deciphering the transcriptional network of the dendritic cell lineage, *Nat Immunol* **13**, 888–899 (2012).
93. A. Musumeci, K. Lutz, E. Winheim, A. B. Krug, What Makes a pDC: Recent Advances in Understanding Plasmacytoid DC Development and Heterogeneity, *Front. Immunol.* **10** (2019), doi:10.3389/fimmu.2019.01222.
94. C. S. Moniaga, S. Watanabe, T. Honda, S. Nielsen, M. Hara-Chikuma, Aquaporin-9-expressing neutrophils are required for the establishment of contact hypersensitivity, *Sci Rep* **5**, 1–13 (2015).
95. P. Dwivedi, K. D. Greis, Granulocyte colony-stimulating factor receptor signaling in severe congenital neutropenia, chronic neutrophilic leukemia, and related malignancies, *Experimental Hematology* **46**, 9–20 (2017).
96. M. Nowicka, C. Krieg, H. L. Crowell, L. M. Weber, F. J. Hartmann, S. Guglietta, B. Becher, M. P. Levesque, M. D. Robinson, CyTOF workflow: differential discovery in high-throughput high-dimensional cytometry datasets, *F1000Res* **6**, 748 (2017).